Broadly tunable mid-infrared noise-immune cavity-enhanced optical heterodyne molecular spectrometer

Michael W. Porambo, Brian M. Siller, Jessica M. Pearson, and Benjamin J. McCall*

Department of Chemistry, University of Illinois at Urbana-Champaign, 600 South Mathews Avenue, Urbana, Illinois 61801, USA
**Corresponding author: bjmccall@illinois.edu*

Received August 10, 2012; revised September 20, 2012; accepted September 20, 2012;
posted September 21, 2012 (Doc. ID 174130); published October 22, 2012

The sensitive spectroscopic technique noise-immune cavity-enhanced optical heterodyne molecular spectroscopy (NICE-OHMS) has been successfully used in a variety of systems; however, no broadly tunable setup has been developed for the mid-infrared. To this end, we have integrated a difference frequency generation system into a NICE-OHMS setup. Initial optimization and characterization was completed with ro-vibrational spectroscopy of methane. Doppler-broadened frequency-modulated NICE-OHMS spectra were recorded at a sensitivity of 2×10^{-7} cm^{-1} Hz$^{-1/2}$. Sub-Doppler saturation signals (Lamb dips) were also observed using wavelength-modulated NICE-OHMS, achieving a sensitivity of $\sim 6 \times 10^{-9}$ cm^{-1} Hz$^{-1/2}$. © 2012 Optical Society of America

OCIS codes: 300.1030, 300.6320, 300.6460, 300.6380, 300.6390, 300.6340.

Noise-immune cavity-enhanced optical heterodyne molecular spectroscopy (NICE-OHMS) is the most sensitive direct absorption technique developed. First reported by Ye and co-workers [1,2], this technique combines the increased absorption due to path length enhancement of cavity-enhanced absorption spectroscopy [3,4] with the low noise of frequency modulation/heterodyne spectroscopy [5]. Not only does NICE-OHMS allow for high sensitivity detection, but it can also probe sub-Doppler saturation features. Rigorous theoretical analyses of the NICE-OHMS signal, both Doppler-broadened and sub-Doppler, have been reported in several works [6,7]. Variants of NICE-OHMS setups have also been developed, such as wavelength-modulated NICE-OHMS [8] and the ion-specific velocity-modulation NICE-OHMS [9].

Additionally, NICE-OHMS has evolved through its integration with different laser systems. Nd:YAG [2], Ti:sapphire [10], laser diode [11], and fiber-laser [12,13] based NICE-OHMS spectrometers have been built, but little work has been done on NICE-OHMS in the mid-infrared (3–10 μm) spectral region. To our knowledge, the only setup reported in this wavelength range is based on a quantum cascade laser (QCL) [14]. QCLs, however, suffer from limited tunability.

Other laser systems offer broader tunability in the mid-infrared. Difference frequency generation (DFG) produces a beam at the frequency difference between two input lasers using a nonlinear crystal, with the tunability only limited by the most tunable of the lasers and the transparency of the crystal. Similarly, continuous wave optical parametric oscillators (cw OPOs) emit mid-infrared radiation tunable from ~2.3 to 4.6 μm. To extend its tunability in the mid-infrared, we have integrated NICE-OHMS with a DFG setup, enabling use of this unique, high-sensitivity spectroscopy continuously in the ~2.8–4.8 μm region.

The experimental setup is illustrated in Fig. 1. A ring Ti:sapphire laser (Sirah-Matisse TS) whose wavelength is measured with a Bristol 621A-IR wavemeter is sent through a double-pass acousto-optic modulator (AOM) [15] that is resonant at ~85 MHz, which redshifts the laser by ~170 MHz and results in no change to the beam pointing upon altering the AOM driving frequency. A Nd:YAG laser (1064 nm) is passed through two electro-optic modulators (EOM). The first EOM (New Focus 4003, MgO:LiNbO$_3$) is resonant at ~112.5 MHz and generates sidebands at the cavity free spectral range used for heterodyne detection; the modulation index is 0.79. The second EOM (ThorLabs EO-PM-NR-C1, MgO:LiNbO$_3$) produces additional sidebands at ~6 MHz, which are used to generate the error signal in a Pound–Drever–Hall locking scheme [16]. The processed error signal is split into two correction pathways. Slow corrections (up to 70 Hz) are sent to the cavity piezoelectric transducer, while fast corrections (up to 60 kHz) are sent to the voltage controlled oscillator (VCO) of the AOM. The Ti:sapphire and Nd:YAG are combined in a periodically poled lithium niobate (PPLN) crystal, which results in a mid-infrared beam at the difference between the frequencies of the two input lasers. This beam can be tuned between 2.8 and 4.8 μm by tuning the Ti:sapphire laser frequency (for NICE-OHMS, the wavelength-dependent reflectivity of the optical cavity mirrors limits the tuning range to 3.0–3.4 μm, but multiple mirror sets could be used to extend the tunability to 2.8–4.8 μm).

The mid-IR DFG is then coupled into a cavity with a finesse of ~300. The cavity transmission is captured

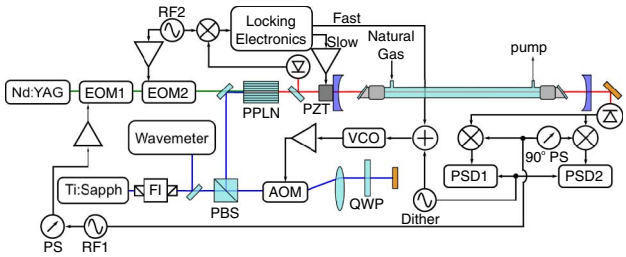

Fig. 1. (Color online) Experimental layout. FI, Faraday isolator; PBS, polarizing beam splitter; AOM, acousto-optic modulator; QWP, quarter-wave plate; VCO, voltage controlled oscillator; EOM, electro-optic modulator; PZT, piezoelectric transducer; RF, radio frequency generator; PS, phase shifter; PSD, phase sensitive detector; PPLN, periodically poled lithium niobate crystal; Δ, amplifier.

on a 120 MHz bandwidth InSb detector (Kolmar). Then, the signal is split and demodulated with two RF mixers that are both referenced to the heterodyne RF frequency, but are 90° out of phase with one another to separate the absorption and dispersion signals.

The sample cell used in this work was equipped with turbomolecular pumps and operated as a flow cell. Natural gas was leaked into the cell from the building supply. Light was coupled through CaF_2 Brewster windows on either end of the cell, which was isolated from the cavity mirrors to reduce vibrational noise.

Two different modulation techniques were performed during this work. The first was frequency modulated (fm)-NICE-OHMS. The second was wavelength modulated (wm)-NICE-OHMS, in which a 50 Hz dither was applied to the AOM VCO to induce a peak-to-peak modulation of 1.7 MHz, and phase sensitive detectors (that is, lock-in amplifiers) demodulated the resulting signal.

Demonstration and characterization of the DFG NICE-OHMS system was conducted by ro-vibrational spectroscopy of methane in natural gas. The heterodyne phase was adjusted such that one mixer output would be approximately tuned to the absorption phase and the other approximately tuned to the dispersion phase. A representative Doppler-broadened spectrum of a methane ro-vibrational transition (containing the absorption and dispersion channels) is shown in Fig. 2.

A fit equation based on Eq. 1 of Ref. [17] was used to fit the data:

$$S = y_0 + A[(\chi_{-1}^{\text{abs}} - \chi_1^{\text{abs}})\cos\ \theta + (2\chi_0^{\text{disp}} - \chi_1^{\text{disp}} - \chi_{-1}^{\text{disp}})\sin\ \theta], \quad (1)$$

where

$$\chi_j^{\text{abs}} = \frac{1}{\sqrt{1+G}} e^{-x^2}, \quad (2)$$

$$\chi_j^{\text{disp}} = \frac{2}{\sqrt{\pi}} e^{-x^2} \int_0^x e^{t^2}\,\mathrm{d}t, \quad (3)$$

and $x = \frac{2\sqrt{\ln 2}(\Delta\nu + j\nu_m)}{\delta\nu}$. Furthermore, θ is the heterodyne detection phase, A is the amplitude, G is the saturation parameter, y_0 is an offset parameter, $\Delta\nu = \nu - \nu_0$ is the detuning of the DFG frequency ν from the transition line center ν_0, ν_m is the heterodyne modulation frequency, and $\delta\nu$ is the transition line width (FWHM). A global analysis fit was performed on both channels simultaneously with θ, ν_m, G, and A constrained to be equal for both detection channels and y_0 allowed to float independently. ν_m is held fixed at 112.5 MHz.

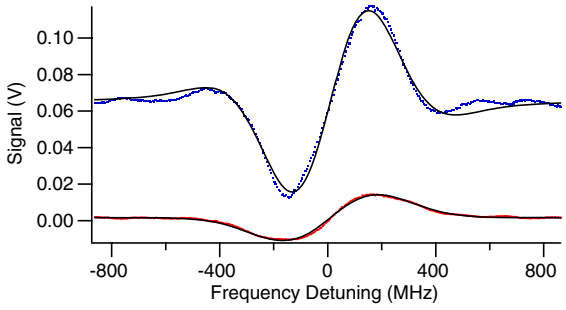

Fig. 2. (Color online) Doppler-broadened fm-NICE-OHMS dispersion (top) and absorption (bottom) signals from the P(9) A_2 transition of the ν_3 fundamental band of CH_4 at a pressure of $\sim 6 \times 10^{-5}$ Torr. Raw data are given as dots, fits to the data are given in solid curves. The dispersion curve is offset vertically for clarity.

The fractional noise equivalent absorption (NEA) is calculated to be $\sim 1 \times 10^{-6}$ cm^{-1} Hz$^{-1/2}$ and $\sim 2 \times 10^{-7}$ cm^{-1} Hz$^{-1/2}$ for the dispersion and absorption detection channels, respectively. Low frequency noise is observed in the baseline, which appears to be phase-dependent; this noise is more pronounced in the dispersion channel than in the absorption channel. This noise is suspected to be from etalons in the optical setup, residual amplitude modulation due to the heterodyne EOM, or a combination of these. Both of these effects can be phase-dependent [18,19], which may explain why one channel contains more noise. Attenuation of the absorption signal due to optical saturation is observed, consistent with published theoretical descriptions [6]. The saturation parameter was determined to be ~70 by the global fit to the data.

Not only does this optical saturation attenuate the Doppler-broadened signal amplitude [6], but it also leads to sub-Doppler Lamb dips. The Lamb dips are the result of two modes of the phase-modulated light (a forward-propagating mode and a counter-propagating mode) interacting with the same velocity group of molecules. Lamb dips are observed in the Doppler-broadened spectrum at the line center for dispersion signals and at multiples of half the heterodyne frequency for both dispersion and absorption. As generally the center dispersion Lamb dip is the strongest of the Lamb dips, the scan parameters were varied to maximize the amplitude of this Lamb dip. Optimization of the center dispersion Lamb dip was aided by the fact that no Lamb dip at line center should be observed in the absorption detection phase; thus, the heterodyne phase was varied until the center Lamb dip in one detection channel was completely eliminated. An optimized center dispersion Lamb dip is shown in Fig. 3.

The sub-Doppler signals were obtained using wm-NICE-OHMS, as described earlier. Wavelength modulation broadened the sub-Doppler line shape sufficiently to observe the signal while taking ~350 kHz steps on the DFG (by tuning the Ti:sapphire laser). This detection scheme also results in higher sensitivity than that of

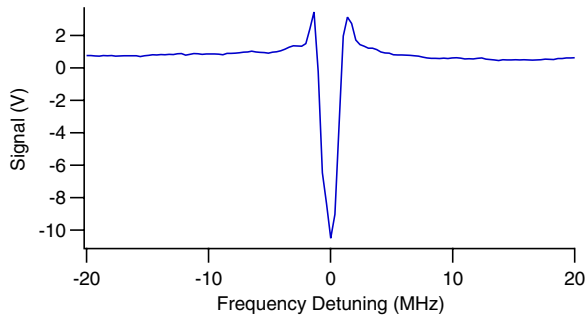

Fig. 3. (Color online) Center dispersion Lamb dip of the P(12) A_1 transition of the ν_3 fundamental band of CH_4 observed at a pressure of $\sim 6 \times 10^{-5}$ Torr.

fm-NICE-OHMS. With wm-NICE-OHMS, the NEA is calculated to be 6×10^{-9} $cm^{-1} Hz^{-1/2}$, which is about 250 times the shot noise limit. This value is about a factor of 60 less sensitive than what was observed for the QCL-based NICE-OHMS spectrometer [14].

Several issues seem to impact the ultimate sensitivity and performance of the spectrometer. Etalons formed between the transmission detector and the optical cavity and between the optical cavity and the DFG PPLN crystal decrease the sensitivity. For the Doppler-broadened scans, these etalons were significantly mitigated by using heat guns across the respective beam paths and averaging for ~1 s per point, as accomplished in [20]. Furthermore, the line shapes of the signals are somewhat distorted by drifts in the frequencies of the pump and signal lasers of the DFG process. To prevent this drifting in the future, we plan to stabilize the frequencies of both lasers by locking the Nd:YAG to an iodine hyperfine transition and the Ti:sapphire to an optical frequency comb.

In summary, we present the first broadly tunable NICE-OHMS spectrometer in the mid-infrared. Coherent mid-infrared radiation is produced through DFG with a Nd:YAG laser and a tunable Ti:sapphire laser combined in a PPLN crystal. The instrument was characterized and optimized by probing ro-vibrational transitions of methane present in natural gas. Doppler-broadened fm-NICE-OHMS absorption and dispersion signals were acquired and fit. Sub-Doppler signals were observed using wm-NICE-OHMS. We have recently integrated this DFG NICE-OHMS system to the fast ion beam spectrometer described in [21]. Additionally, our research group has completed development of a similar mid-infrared NICE-OHMS system based on a cw OPO [22]. Both of these systems will be used to study ro-vibrational spectra of molecular ions.

The authors wish to thank Craig Riccardo and Joe Puhr for their help in acquiring spectra for this study. This work has been supported by the National Science Foundation (PHY-08-55633), the NASA Laboratory Astrophysics program (NNX08AN82G), and a David and Lucile Packard Fellowship. M. W. Porambo has been supported by a Robert C. and Carolyn J. Springborn Fellowship from the University of Illinois.

References

1. J. Ye, "Ultrasensitive high resolution laser spectroscopy and its application to optical frequency standards," Ph.D. thesis (University of Colorado at Boulder, 1997).
2. J. Ye, L. Ma, and J. Hall, J. Opt. Soc. Am. B **15**, 6 (1998).
3. R. Engeln, G. Berden, R. Peeters, and G. Meijer, Rev. Sci. Instrum. **69**, 3763 (1998).
4. K. Anzai, X. Gao, H. Sasada, and N. Yoshida, Jpn. J. Appl. Phys. **45**, 2771 (2006).
5. G. C. Bjorklund and M. D. Levenson, Appl. Phys. B **32**, 145 (1983).
6. W. Ma, A. Foltynowicz, and O. Axner, J. Opt. Soc. Am. B **25**, 1144 (2008).
7. O. Axner, W. Ma, and A. Foltynowicz, J. Opt. Soc. Am. B **25**, 1166 (2008).
8. N. J. van Leeuwen and A. C. Wilson, J. Opt. Soc. Am. B **21**, 1713 (2004).
9. B. M. Siller, M. W. Porambo, A. A. Mills, and B. J. McCall, Opt. Express **19**, 24822 (2011).
10. L. S. Ma, J. Ye, P. Dube, and J. L. Hall, J. Opt. Soc. Am. B **16**, 2255 (1999).
11. C. Ishibashi and H. Sasada, Jpn. J. Appl. Phys. Part 1 **38**, 920 (1999).
12. F. M. Schmidt, A. Foltynowicz, W. Ma, and O. Axner, J. Opt. Soc. Am. B **24**, 1392 (2007).
13. F. M. Schmidt, A. Foltynowicz, W. Ma, T. Lock, and O. Axner, Opt. Express **15**, 10822 (2007).
14. M. S. Taubman, T. L. Myers, B. D. Cannon, and R. M. Williams, Spectrochim. Acta A **60**, 3457 (2004).
15. E. A. Donley, T. P. Heavner, F. Levi, O. Tataw, and S. R. Jefferts, Rev. Sci. Instrum. **76**, 063112 (2005).
16. R. W. P. Drever, J. L. Hall, F. V. Kowalski, J. Hough, G. M. Ford, A. J. Munley, and H. Ward, Appl. Phys. B **31**, 97 (1983).
17. A. Foltynowicz, F. M. Schmidt, W. Ma, and O. Axner, Appl. Phys. B **92**, 313 (2008).
18. E. A. Whittaker, M. Gehrtz, and G. C. Bjorklund, J. Opt. Soc. Am. B **2**, 1320 (1985).
19. N. C. Wong and J. L. Hall, J. Opt. Soc. Am. B **2**, 1527 (1985).
20. J. F. Kelly, R. L. Sams, T. A. Blake, M. Newburn, and J. Moran, Rev. Sci. Instrum. **83**, 023101 (2012).
21. A. A. Mills, B. M. Siller, M. W. Porambo, M. Perera, H. Kreckel, and B. J. McCall, J. Chem. Phys. **135**, 224201 (2011).
22. K. N. Crabtree, J. N. Hodges, B. M. Siller, A. J. Perry, J. E. Kelly, P. A. Jenkins II, and B. J. McCall, "Sub-Doppler mid-infrared spectroscopy of molecular ions," Chem. Phys. Lett. (to be published).